RSC Advances

RSC Publishing

PAPER

View Article Online
View Journal | View Issue

Cite this: *RSC Adv.*, 2013, **3**, 22008

Encapsulation of lipase in mesoporous silica yolk–shell spheres with enhanced enzyme stability†

Zheng Yang Zhao,[a] Jian Liu,*[b] Mandy Hahn,[a] Shizhang Qiao,*[c] Anton P. J. Middelberg[d] and Lizhong He*[a]

Received 3rd July 2013
Accepted 19th August 2013

DOI: 10.1039/c3ra43382j

www.rsc.org/advances

Enzyme encapsulation is an attractive method among the different immobilization strategies to improve the reusability and stability of enzymes because it can separate enzymes from a hazardous external environment. However, current encapsulation methods have limitations including enzyme leakage. In this study, a new approach based on a two-step soft templating method has been proposed to encapsulate lipase within substrate permeable mesoporous silica yolk–shell spheres. In the first step, lipase was immobilized onto epoxy functionalized silica nanospheres that serve as the core materials. The core materials were mixed with a fluorocarbon surfactant, FC4, to form a core–vesicle complex. In the second step, a mesoporous silica shell was assembled surrounding the core–vesicle complex to form the yolk–shell structure with the lipase encapsulated. The mesoporous silica shell has a pore size of 2.1 nm, which is permeable to the reactant and product while isolating the enzymes from harmful external conditions. The encapsulated lipase retained 87.5% of its activity after thermal treatment at 70 °C for 2 hours while the free enzyme lost 99.5% of its activity under the same treatment. Importantly, the encapsulated lipase shows significantly enhanced resistance to degradation by proteases.

Introduction

Enzymes are excellent biocatalysts and are widely used in modern industry.[1] However, enzymes are instable towards heat, organic solvents, acids or bases, and are difficult to recycle.[2] Therefore, robust immobilisation of enzymes is very important for their wide spread application because of the increased ease of separation, and the potential to improve the recyclability and stability.[3] Increasing stability allows enzymes to be applied widely in industry, particularly under extreme conditions, such as high temperature, extreme pH and in complex biological environments. Various methods such as physical adsorption,[4] covalent chemical binding,[5,6] crosslinking[7] and encapsulation[8] have been developed for the immobilisation of enzymes. Among these methods, encapsulation has been widely used, as it can avoid structural changes of the enzymes while separating them from hazardous external environments.[9] Thus, an independent microenvironment inside the capsules can be constructed to remove the enzyme from an extreme external environment.

Enzyme encapsulation has been applied in many different materials. For instance, lactate dehydrogenase has been encapsulated into a nanoporous silica sol–gel glass,[6] however, as the size of the surface pore was very large (30 nm) and protection of enzyme was not efficient, only limited stability was achieved.[6] κ-Carrageenan, has also been used for enzyme encapsulation.[10] However, the stability of κ-carrageenan is not high enough and it cannot work at temperatures higher than 50 °C.[10] Therefore, the encapsulated enzyme cannot be used in extreme industrial conditions. Enzymes encapsulated by a sol–gel polymer[11] show good activity, but the wide pore-size distribution in sol–gel polymers cannot be controlled well, and this adversely influences the diffusion of reactants and products during biocatalysis to the detriment of their practical application.

Enzyme encapsulation can be achieved using different methods such as a sol–gel process or bio-inspired encapsulation.[9,12] Silica-based sol–gel encapsulation is the most used technique for enzyme encapsulation, particularly for the development of biosensors, because silica can provide a high specific surface area and controllable pore diameter.[8,13] However, the sol–gel method has limitations including poor loading efficiency and enzyme leakage.[12] Bio-inspired enzyme encapsulation can be carried out using biomimetic mineral formation, producing inorganic carrier matrices for enzyme

[a]*Department of Chemical Engineering, Monash University, Clayton, VIC 3800, Australia. E-mail: lizhong.he@monash.edu*

[b]*Department of Chemical Engineering, Curtin University, Perth, WA 6845, Australia. E-mail: jian.liu@curtin.edu.au; Tel: +61 8 92662522*

[c]*School of Chemical Engineering, The University of Adelaide, Adelaide, SA 5005, Australia. E-mail: s.qiao@adelaide.edu.au*

[d]*Centre for Biomolecular Engineering, Australian Institute for Bioengineering and Nanotechnology and School of Engineering, The University of Queensland, St Lucia, Brisbane, QLD 4072, Australia*

† Electronic supplementary information (ESI) available: Activity analysis of lipase, cleavage site of lipase by proteinase K, and lysine residues on a lipase surface. See DOI: 10.1039/c3ra43382j

immobilization, and such matrices are typically based on silica.[12] However, this method still faces significant hurdles in controlling silica encapsulation *in vitro*, in part, due to a lack of understanding of the mineral formation mechanism.

In order to overcome the drawbacks of these conventional encapsulation methods, different encapsulation methods have been developed. For instance, a layer-by-layer assembly based on polyelectrolytes has been used to encapsulate an enzyme adsorbed on a nanoparticle,[14,15] in which the polyelectrolyte shell can prevent leakage of the enzymes and protect them from the proteolysis of protease. The surfactant cetyltrimethylammonium bromide (CTAB) has also been reported to encapsulate an enzyme adsorbed on silica particles, improving enzyme stability.[16] In these methods, the encapsulation layers are physically adsorbed onto the nanoparticles, and the stability of these layers is affected by solution conditions. The encapsulated enzymes are thus vulnerable to leaking induced by changes of the solution conditions.

Silica-based mesoporous materials have attractive properties including variable pore size and large pore volume for catalytic applications.[17–19] Efforts have been made to use mesoporous silica to achieve high enzyme loading for enzyme immobilization.[20,21] Recently, mesoporous shell structured silica nanoparticles[22] with various catalysts have been synthesised as nanoreactors for several reactions.[23] Silica shells can prevent aggregation of the catalysts, meanwhile, allowing small molecules access to the hollow space inside for effective catalytic reactions. These recent advances of mesoporous silica shells make it possible to encapsulate enzymes into a yolk–shell structure, with the silica shell serving as a robust and stable encapsulation layer to protect the enzymes.

In this study a two-step soft templating method has been developed for the encapsulation of lipase from *Thermomyces lanuginosus* into a mesoporous silica yolk–shell sphere (MSYS). In the first step, lipase was immobilised onto an epoxy-functionalised silica nanoparticle (EFSN) that served as the core material. In the next step, a porous silica shell was formed on the lipase-immobilized silica nanoparticles. The activity and stability of the encapsulated lipase were compared with those of the free enzyme.

Material and methods

Materials

Lipase from *Thermomyces lanuginosus* (L0777), *para*-nitrophenyl palmitate (*p*npp) (N2752), ammonium hydroxide solution (338818), tetraethyl orthosilicate ($Si(OC_2H_5)_4$ (TEOS) (>99%), 3-glycidoxypropyltrimethoxysilane (3-GPS, 2530-83-8), *para*-nitrophenol (*p*np) grade (1048), gum Arabic (G9752), Triton-X-100 (X100), sodium chloride (S7653), Trizma® base (T1503), sodium carbonate (S7795), hydrochloric acid (320331) and ethanol amine (110167) were purchased from Sigma-Aldrich (Sydney, Australia). Fluorocarbon surfactant FC4, $[C_3F_7O(CFCF_3CF_2O)_2CF\text{-}CF_3CONH(CH_2)_3N^+(C_2H_5)_2CH_3]I^-$, was obtained from Yick Vic Chemicals (Hong Kong). Water (a resistivity of 18.2 MΩ cm) was purified using a Milli-Q system.

Epoxy group functionalization

Epoxy functionalization of silica nanospheres was carried out using the method previous reported by Liu *et al.*[24] 1 g silica nanospheres (SNs) was added into 100 ml of toluene. The mixture was firstly sonicated for 40 minutes to facilitate dispersion, and then 1.6 ml of (3-glycidyloxypropyl)trimethoxysilane was added. The mixture was refluxed at 70 °C for 24 h. The solid products were centrifuged, washed with toluene and methanol sequentially and repeated three times and air dried in oven at 60 °C for two days.

Lipase immobilisation on silica nanospheres

Lipase immobilised silica nanospheres (LISNs) were synthesized by following the procedure below: 200 mg EFSN was mixed with 1 ml free lipase (6.1 mg ml^{-1} in 50 mM carbonate buffer, pH 9.5) and incubated overnight with 250 rpm shaking at 37 °C. After collecting the supernatant for analysis of the concentration of the remaining lipase, the LISNs were washed with NaCl solution (1 M) and water sequentially and repeated 3 times, this was followed by a blocking step using ethanolamine (1.0 M, pH 9) and then another wash with water. Then, the LISNs were dispersed in Tris–HCl buffer (50 mM, pH 8) to make a 10 mg ml^{-1} solution.

Synthesis of lipase-encapsulated mesoporous silica yolk–shell spheres

A silica porous layer was coated onto the LISNs to form the lipase-encapsulated mesoporous silica yolk–shell spheres (LEMSYSs) as follows: 1.5 ml LISNs (10 mg ml^{-1}) in Tris–HCl buffer (50 mM, pH 8) was mixed with 48 mg fluorocarbon surfactant FC4, 4.5 ml H_2O, 2 ml ethanol and 0.05 ml 28–30% NH_4OH. After incubating with stirring at 30 °C for 4 hours, 0.11 g TEOS was added to initiate the coating of the silica layer, and the reaction was left for 20 hours. The temperature was then raised to 60 °C and incubated for 24 hours. Drying of the samples was realized by opening the container in an oven at 60 °C, and evaporation was carried out for 24 hours. The LEMSYS product was re-suspended in 1.5 ml Tris–HCl buffer (50 mM, pH 8), and was washed with the same buffer before storage.

Material characterisation

Nitrogen sorption isotherms of the samples were measured by a micromeritics ASAP 2020 surface area and porosity analyser at 77 K. Prior to the measurement, the sample was degassed at 90 °C for 8 hours. The Brunauer–Emmett–Teller (BET) specific surface areas were calculated using adsorption data at a relative pressure range of $P/P_0 = 0.05$–0.3. Pore size distributions were derived from the adsorption branch using the Barrett–Joyner–Halenda (BJH) method. The total pore volumes were estimated from the amounts adsorbed at a relative pressure (P/P_0) of 0.99.

TEM images were obtained using a JEOL JEM 2100 electron microscope. The powder samples for the TEM measurements were suspended in ethanol and then dropped onto Cu grids with holey carbon films. SEM images were obtained using a

JEOL 7001F electron microscope. The powder samples were placed on carbon tape and coated with 1 nm platinum for SEM measurements.

FT-IR measurement was carried out using a PerkinElmer Spectrum 100 FT-IR spectrometer from 500 cm^{-1} to 4000 cm^{-1} using potassium bromide as a background. The scan was repeated 20 times.

Lipase concentration and activity test

Protein concentration was detected with a Pierce 660 nm protein assay (Thermo Scientific, Melbourne, Australia) using bovine serum albumin (BSA) as a standard. 100 μl protein solution was added into 1.5 ml assay reagent and the mixture was left to react for 5 min. Then, absorbance at 660 nm was measured by a UV spectrometer. The lipase concentration on the nanospheres was determined by mass balance (concentration change of lipase in the supernatant before and after immobilization).

The lipase activity was determined using the modified method of Winkler.[25] Briefly, the method used *para*-nitrophenyl palmitate as a substrate[25] (reaction mechanism shown in Fig. S1†) and Triton-X-100 as a surfactant[26] to help dissolve the unreacted substrate. In a 15 ml falcon tube, 1.8 ml reaction buffer (50 mM Tris–HCl pH 8 in the presence of 0.4% Triton X-100) was mixed with 0.2 ml substrate solution (10 mM substrate in 2-propanol) and 0.2 ml sample (either free lipase solution or LEMSYS solution; for control, 0.2 ml Tris buffer was added), and incubated in a 35 °C water bath with 200 rpm shaking. After 20 minutes of incubation, the concentration of the product *p*np was determined by measuring the absorbance at 404 nm. One unit of lipase activity was defined as production of 1 μmol of *p*np per min. Thermal stability was determined by comparing lipase activity before and after heat treatment (70 °C in an oven for 2 hours).

Proteinase K degradation resistance was determined by residual activity after treatment. Proteinase K degradation resistance was determined by an activity test after mixing samples with proteinase K solution (3.5 mg ml^{-1} in 50 mM Tris–HCl buffer, pH 8) at a volume ratio of 1 : 1 under 37 °C for 20 minutes. Then, the lipase activity of all the samples was determined and compared with the original activity before proteinase K treatment.

Results and discussion

The synthesis of the enzyme-encapsulated yolk–shell structured materials is schematically represented in Fig. 1, and the process comprises of two steps. In the first step, solid silica spheres with diameters around 320 nm are selected as core materials, and their conjugation with lipase was achieved using functional epoxy groups on the silica surfaces. Then, the lipase-coated silica nanospheres were mixed with a fluorocarbon surfactant $[C_3F_7O(CFCF_3CF_2O)_2CFCF_3CONH(CH_2)_3N^+(C_2H_5)_2CH_3I^-]$, (FC4) to form vesicles. In the second step, hybrid silane–surfactant micellar aggregates, which are built of hydrolysed/oligomerised TEOS species and FC4, assemble under basic conditions while

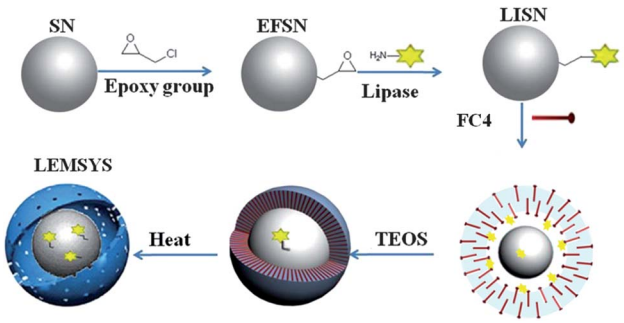

Fig. 1 Schematic illustration of the formation of a lipase-encapsulated mesoporous silica yolk–shell sphere (LEMSYS). SN: silica nanosphere, EFSN: epoxy functionalized silica nanosphere, LISN: lipase-immobilized silica nanosphere.

surrounding the core–vesicle complex and eventually form an ordered mesostructured organosilica shell *via* cooperative self-assembly. Following further growth and a ripening process of the shell, induced by condensation of the silica oligomeric species, a mesoporous silica yolk–shell structure can be obtained after removal of the FC4 templates by heating at 60 °C and drying. The material thus-obtained is denoted as LEMSYS, which consists of an enzyme-immobilized silica core, hollow space between core and shell, and mesoporous silica shell.

The silica sphere cores prepared by the Stober method have a narrow size distribution with diameters of 320 nm as observed from their SEM images (Fig. 2). FT-IR spectra of epoxy functionalised silica spheres showed a C–H stretching band at 2850–2950 cm^{-1} and 1639 cm^{-1} along with the Si–C band at 1120–1220 cm^{-1} (Fig. 3), confirming that the epoxy group has been grafted onto the silica core.

Fig. 4 shows representative TEM images of LEMSYSs presenting a 320 nm silica core, the 70 nm hollow void and a mesoporous shell with 20–30 nm thickness. The overall outer diameter is 440 nm for a single yolk–shell sphere (Fig. 4a). A high resolution transmission electron microscopy image of a LEMSYS, as shown in Fig. 4b, further confirms the mesopores in the shell, with the voids on the silica core observed. Further evidence of the mesoporous structure of the LEMSYS can be

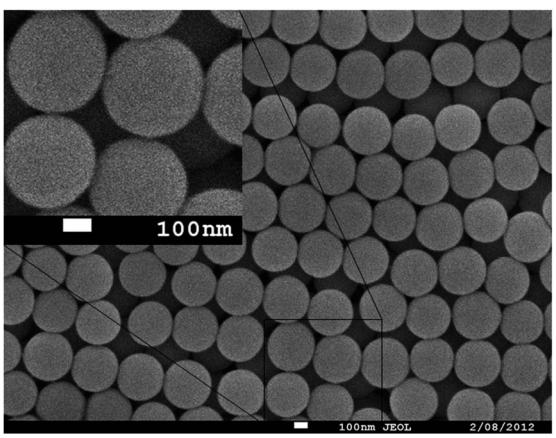

Fig. 2 SEM image of silica nanospheres (SN).

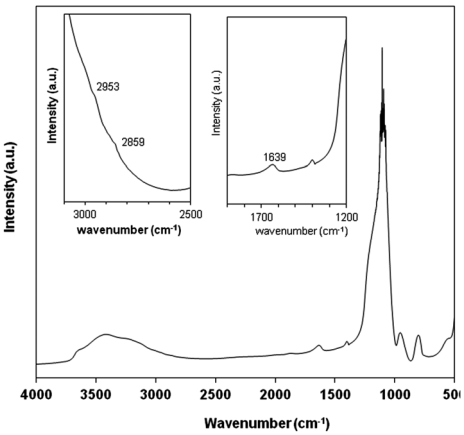

Fig. 3 FT-IR characterization of epoxy functionalized silica nanospheres (EFSN).

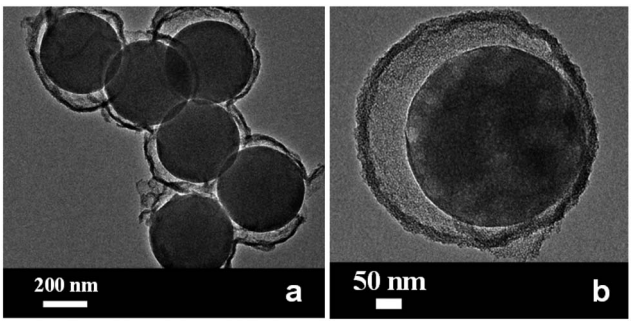

Fig. 4 TEM images of LEMSYSs.

obtained by the N_2 sorption analysis. The adsorption–desorption isotherm obtained on LEMSYS shows a type IV behaviour with a two-step capillary condensation in the relative pressure ranges of 0.1–0.3 and 0.7–0.9 (see Fig. 5a), in agreement with the presence of a hierarchical porosity organisation consistent with the yolk–shell structure. The Barrett–Joyner–Halenda (BJH) pore size distribution shows two peaks (see Fig. 5b), corresponding to the mesopores of the shell (2.1 nm) and the void between the solid core and the shell (4.4 nm). In addition, the Brunauer–Emmett–Teller (BET) specific surface area and total pore volume are calculated to be 151 $m^2\ g^{-1}$ and 0.18 $cm^3\ g^{-1}$, respectively.

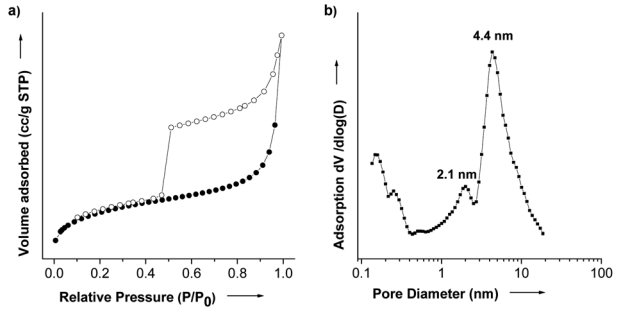

Fig. 5 Nitrogen adsorption isotherm and the BJH pore size distribution of LEMSYSs. (a) Nitrogen adsorption isotherm and (b) BJH pore size distribution.

After immobilization, the protein concentration in the supernatant was tested with a Pierce 660 nm protein assay by using bovine serum albumin (BSA) as a standard. The calculation based on mass balance shows that the concentration of immobilized lipase is *ca.* 11 mg per gram of EFSN. This is a modest immobilization ratio because solid silica spheres rather than porous particles have been used for immobilization. As immobilization of lipase on EFSNs is based on a covalent reaction between the primary amines of the lysine residues of lipase and the epoxy group on EFSNs, the conjugation between silica spheres and lipase is very stable. After synthesis of the LEMSYSs, the particles were suspended in Tris buffer (50 mM, pH 8), and no leaked protein was detected in the suspension buffer.

The lipase activity of free lipase and LEMSYSs were investigated by using *para*-nitrophenyl palmitate as a substrate[25] and Triton-X-100 as a surfactant[26] to facilitate the dissolution of the unreacted substrate. In Fig. 6, the time courses of the hydrolysis reaction catalysed by free and encapsulated lipases are compared at the same lipase concentration. It is obvious that lipase activity has been decreased after two steps of synthesis. As seen in Table S1,† activity of encapsulated lipase (0.75 U mg^{-1}) is lower than that of the free enzyme (4.7 U mg^{-1}). Despite this drawback, lipase's reusability and stability have been significantly improved as shown below.

The reusability of encapsulated lipase is shown in Fig. 7. In the second and the third reuse cycles, the activities have decreased to 60.3% and 43.6% of the initial activity, respectively. After these two quick decreases, the activity is reasonably stable (35–31.6%) in the range of 3–6 reuse cycles. As we used centrifugation to recover the LEMSYSs, it is expected that some LEMSYSs may have been lost during each cycle, and the true loss of enzyme activity may be lower than that shown in Fig. 7.

Encapsulated lipase also has enhanced thermal stability. The thermal stability of free lipase and LEMSYSs was examined by comparing lipase activity before and after thermal treatment (incubation in an oven at 70 °C for 2 hours). As shown in Fig. 8a, the thermal stability of encapsulated lipase is about 170 times higher than that of free lipase. The increase of lipase stability by encapsulation in this work is consistent with those reported in

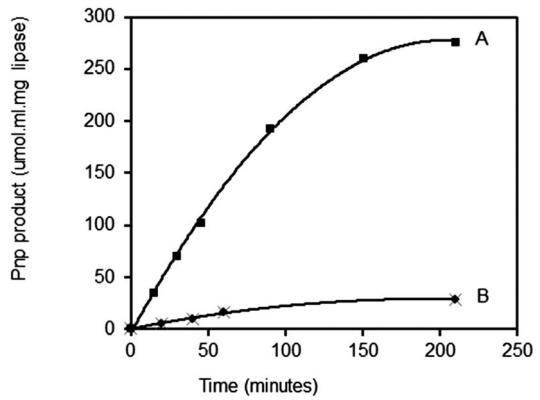

Fig. 6 Comparison of the hydrolysis reaction catalysed by (A) free lipase and (B) encapsulated lipase.

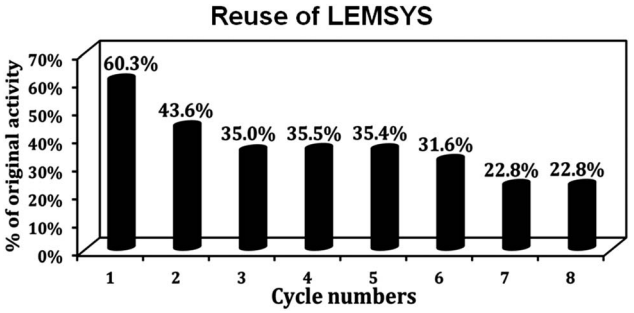

Fig. 7 Reusability of the encapsulated lipase.

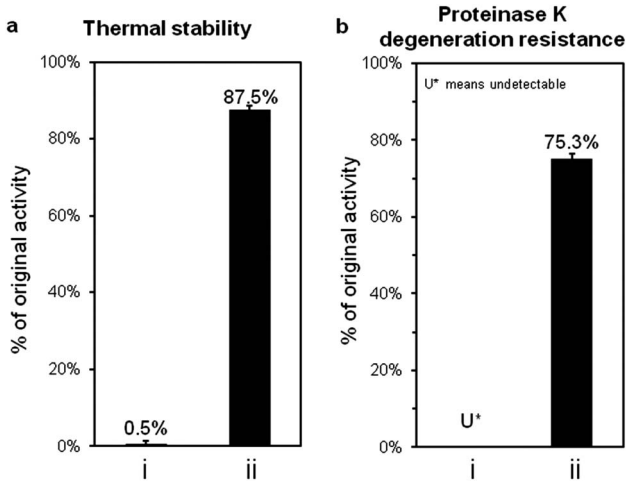

Fig. 8 The thermal stability and proteinase K degeneration resistance of free and encapsulated lipase. (i) Free lipase, and (ii) lipase encapsulated in a yolk–shell sphere. The value of the percentage was the remaining lipase activity after thermal treatment (a) or mixing with proteinase K (b), divided by the activity before the treatment.

the literature.[27–30] There are different factors that may contribute to the enhanced stability. First, the lipase has multiple lysine residues on it's surface (Fig. S2†), which can form multiple covalent bonds with the silica surface. Such multiple covalent immobilisation may enhance the enzyme rigidification and prevent enzyme aggregation, thus increasing enzyme stability.[30] Second, the porous silica shell may provide additional protection by preventing enzyme–enzyme interactions across different nanoparticles. Furthermore, after encapsulation, the silica shell may provide a microenvironment which might prevent enzymes from thermal damage.

One significant advantage of a yolk–shell structure is that the shell can isolate the enzyme from harmful conditions, such as exposure to proteases. The proteolysis vulnerability of the lipase was tested by mixing free lipase or LEMSYSs with proteinase K, a proteinase widely used to proteolyse peptides and proteins. The cleavage site of lipase by proteinase K can be found in the ESI (Fig. S2†). One volume of sample was mixed with one volume of proteinase K solution (3.5 mg ml^{-1} in 50 mM Tris–HCl buffer, pH 8) and incubated at 37 °C for 20 minutes before activity measurement. As shown in Fig. 8b, free lipase lost its entire activity after being exposed to proteinase K, with no detectable activity. In contrast, the encapsulated lipase in LEMSYSs maintained 75% of its activity. Although the silica shell of the LEMSYSs significantly increases the lipase stability against proteolysis, it does not provide 100% protection from the proteinase. This vulnerability may be caused by a few large pores in the silica shells, through which the proteinase K can attack the encapsulated lipases. Nevertheless, the protective function of the silica shell is significant, demonstrating that the yolk–shell structure plays an important role in improving the enzyme stability.

While achieving significantly enhanced enzyme stability by encapsulation, there is a notable decrease of enzyme activity which deserves further discussion. We recognize activity loss can occur in both steps of the synthesis. In the first step of lipase immobilization, lipase was covalently bound to silica spheres. There are 7 lysine residues on the surface of lipase (Fig. S2†). As the reaction of the lysine residues with epoxy groups is random, some lipase may have their functional sites buried and cannot properly come into contact with the substrate, thus decreasing activity. In the second step, removal of the template was carried out at 60 °C and the samples were dried for 24 h. This modified condition is relatively mild, compared to the experimental conditions (550 °C for 6 h) used in a previous publication.[22] However, this treatment at high temperature for a long period may cause the enzyme to denature and thus lead to a loss of activity. On the other hand, this mild condition is not expected to fully remove the templates. The existence of un-removed templates may decrease the accessibility of the enzyme to the substrate, thus decreasing the apparent activity of the lipase. Further study is needed to improve the method to better preserve enzyme activity.

Solid silica spheres have been used as core materials in the current work. It is expected that loading of enzymes can be enhanced by using porous silica spheres as core materials, thus improving the efficiency of the core–shell-based enzyme systems. In this work, *para*-nitrophenyl palmitate has been used as a substrate to test lipase activity. Smaller substrates such as triacetin have also been reported by other researchers for evaluation of activity of immobilized lipase.[31] As the pore size in the shells in our system is only 2 nm, it is expected that the activity of lipase will be higher for small substrates like triacetin. We anticipate that enlarging the pore size of the shell can increase lipase activity for *para*-nitrophenyl palmitate. However, caution should be taken to avoid oversized pores, which may lead to an unwanted loss of protection from shells against proteases. Optimization of the pore size is needed in future work to ensure that a high activity and strong protection can be achieved simultaneously.

Conclusions

In conclusion, a two-step soft templating method has been established to encapsulate the enzyme lipase into mesoporous yolk–shell silica. After encapsulation, lipase retains its activity. Compared with the free enzyme, both thermal stability and resistance to protease degradation have been significantly

enhanced. In contrast with the total loss of activity of free lipase after proteinase K degeneration treatment, the encapsulated enzyme still possess 75% of its original activity. This work has demonstrated that it is feasible to use yolk–shell mesoporous silica to encapsulate enzymes. This may open a door to further explore the development of a nano-bioreactor, utilizing the reaction advantages provided by the combination of a nano-structured yolk–shell sphere with enzymes.

Acknowledgements

L.H. acknowledges New Staff start-up funding provided by Department of Chemical Engineering at Monash University. This work was financially supported by the Australian Research Council (ARC) through Discovery Project program (DP1094070). J.L. gratefully acknowledges the award of ARC Australian Post-doctoral Fellowship (APD). The authors thank Ms Wenjie Liu for assistance in SEM measurements.

Notes and references

1 B. Chen, J. Hu, E. M. Miller, W. Xie, M. Cai and R. A. Gross, *Biomacromolecules*, 2008, **9**, 463–471.
2 L. Fjerbaek, K. V. Christensen and B. Norddahl, *Biotechnol. Bioeng.*, 2009, **102**, 1298–1315.
3 U. T. Bornscheuer, *Angew. Chem., Int. Ed.*, 2003, **42**, 3336–3337.
4 C. Mateo, O. Abian, R. Fernandez-Lafuente and J. M. Guisan, *Biotechnol. Bioeng.*, 2000, **68**, 98–105.
5 S. L. Hirsh, M. M. M. Bilek, N. J. Nosworthy, A. Kondyurin, C. G. dos Remedios and D. R. McKenzie, *Langmuir*, 2010, **26**, 14380–14388.
6 A. Buthe, S. T. Wu and P. Wang, *Enzyme Stabilization and Immobilization: Methods and Protocols*, 2011, vol. 679, pp. 37–48.
7 Y. C. Zhang and C. Ji, *Anal. Chem.*, 2010, **82**, 5275–5281.
8 A. C. Patel, S. X. Li, J. M. Yuan and Y. Wei, *Nano Lett.*, 2006, **6**, 1042–1046.
9 U. Hanefeld, L. Gardossi and E. Magner, *Chem. Soc. Rev.*, 2009, **38**, 453–468.
10 K. R. Jegannathan, E. S. Chan and P. Ravindra, *J. Mol. Catal. B: Enzym.*, 2009, **58**, 78–83.
11 Y. Sun and S. Wang, *Bioelectrochemistry*, 2007, **71**, 172–179.
12 L. Betancor and H. R. Luckarift, *Trends Biotechnol.*, 2008, **26**, 566–572.
13 Y. X. Sun and S. F. Wang, *Bioelectrochemistry*, 2007, **71**, 172–179.
14 Y. J. Wang and F. Caruso, *Chem. Mater.*, 2005, **17**, 953–961.
15 Y. J. Wang and F. Caruso, *Chem. Commun.*, 2004, 1528–1529.
16 T. Itoh, R. Ishii, S. Matsuura, J. Mizuguchi, S. Hamakawa, T. Hanaoka, T. Tsunoda and F. Mizukami, *Colloids Surf., B*, 2010, **75**, 478–482.
17 Y. Deng, Y. Cai, Z. Sun, J. Liu, C. Liu, J. Wei, W. Li, C. Liu, Y. Wang and D. Zhao, *J. Am. Chem. Soc.*, 2010, **132**, 8466–8473.
18 J. Wei, Q. Yue, Z. Sun, Y. Deng and D. Zhao, *Angew. Chem., Int. Ed.*, 2012, **51**, 6149–6153.
19 Q. Yue, M. Wang, J. Wei, Y. Deng, T. Liu, R. Che, B. Tu and D. Zhao, *Angew. Chem., Int. Ed.*, 2012, **51**, 10368–10372.
20 S. Urrego, E. Serra, V. Alfredsson, R. M. Blanco and I. Díaz, *Microporous Mesoporous Mater.*, 2010, **129**, 173–178.
21 C. Wu, G. Zhou, X. Jiang, J. Ma, H. Zhang and H. Song, *Process Biochem.*, 2012, **47**, 953–959.
22 J. Liu, S. Z. Qiao, S. Budi Hartono and G. Q. Lu, *Angew. Chem., Int. Ed.*, 2010, **49**, 4981–4985.
23 J. Liu, S. Z. Qiao, J. S. Chen, X. W. Lou, X. R. Xing and G. Q. Lu, *Chem. Commun.*, 2011, **47**, 12578–12591.
24 J. Liu, B. Wang, S. B. Hartono, T. T. Liu, P. Kantharidis, A. P. J. Middelberg, G. Q. Lu, L. Z. He and S. Z. Qiao, *Biomaterials*, 2012, **33**, 970–978.
25 U. K. Winkler and M. Stuckmann, *J. Bacteriol.*, 1979, **138**, 663–670.
26 N. Gupta, P. Rathi and R. Gupta, *Anal. Biochem.*, 2002, **311**, 98–99.
27 A. Dyal, K. Loos, M. Noto, S. W. Chang, C. Spagnoli, K. V. P. M. Shafi, A. Ulman, M. Cowman and R. A. Gross, *J. Am. Chem. Soc.*, 2003, **125**, 1684–1685.
28 M. Kalantari, M. Kazemeini, F. Tabandeh and A. Arpanaei, *J. Mater. Chem.*, 2012, **22**, 8385.
29 H. R. Luckarift, J. C. Spain, R. R. Naik and M. O. Stone, *Nat. Biotechnol.*, 2004, **22**, 211–213.
30 C. Mateo, J. M. Palomo, G. Fernandez-Lorente, J. M. Guisan and R. Fernandez-Lafuente, *Enzyme Microb. Technol.*, 2007, **40**, 1451–1463.
31 C. Wang, G. Zhou, Y. Xu and J. Chen, *J. Phys. Chem. C*, 2011, **115**, 22191–22199.